

Laplacian Smoothing Gradient Descent

Stanley Osher

Department of Mathematics
University of California, Los Angeles
sjo@math.ucla.edu

Bao Wang

Department of Mathematics
University of California, Los Angeles
wangbaonj@gmail.com

Penghang Yin

Math Department
UCLA
yph@ucla.edu

Xiyang Luo

Department of Mathematics
University of California, Los Angeles
xylmath@gmail.com

Minh Pham

Math Department
UCLA
minhrose@math.ucla.edu

Alex Lin

Math Department
UCLA
atlin@math.ucla.edu

March 23, 2022

Abstract

We propose a very simple modification of gradient descent and stochastic gradient descent. We show that when applied to a variety of machine learning models including softmax regression, convolutional neural nets, generative adversarial nets, and deep reinforcement learning, this very simple surrogate can dramatically reduce the variance and improve the accuracy of the generalization. The new algorithm, (which depends on one nonnegative parameter) when applied to non-convex minimization, tends to avoid sharp local minima. Instead it seeks somewhat flatter local (and often global) minima. The method only involves preconditioning the gradient by the inverse of a tri-diagonal matrix that is positive definite. The motivation comes from the theory of Hamilton-Jacobi partial differential equations. This theory demonstrates that the new algorithm is almost the same as doing gradient descent on a new function which (a) has the same global minima as the original function and (b) is "more convex". Again, the programming effort in doing this is minimal, in cost, complexity and effort. We implement our algorithm into both PyTorch and Tensorflow platforms, which will be made publicly available.

1 Introduction

Understanding the generalization capability of deep neural nets (DNNs) has drawn enormous recent attention. Stochastic gradient descent (SGD) defines a family of algorithms that make the training of DNNs practical, and it is believed to somehow implicitly smooth the loss function of the DNNs [14]. Much effort has been carried out to improve the training and generalization of DNNs by directly searching for flat minima. Keskar, et. al. examine the maximum loss in a small neighborhood of the minima to locate the flat minima [15]. Chaudhari, et. al. propose the so-called local entropy loss which convexifies the cross entropy loss function [6]. In a recent paper [7], the authors establish the connections between the local entropy, the Moreau envelope [24] and a Hamilton-Jacobi partial differential equation (HJ-PDE) [9], and propose a stochastic backward Euler algorithm to search for the optimal minimizer for a nonconvex function. This stochastic backward Euler algorithm has also been shown to be very efficient for k -means clustering [30]. An alternative view of SGD's magic comes from the theory of uniform stability [4, 8, 12, 3, 10].

The aforementioned work exploits the local geometry of the landscape, which can be computationally expensive. In this work, we do not explicitly consider the landscape. Instead, we directly apply a carefully designed pre-conditioner to smooth the gradient. We shall refer to this procedure as Laplacian smoothing. The gradient smoothing can be done by solving a

tri-diagonal linear system with the original gradient on the right hand side. More precisely, we simply pre-multiply the gradient by the inverse of the following tri-diagonal convolution matrix

$$A_\sigma = \begin{bmatrix} 1+2\sigma & -\sigma & 0 & \dots & 0 & -\sigma \\ -\sigma & 1+2\sigma & -\sigma & \dots & 0 & 0 \\ 0 & -\sigma & 1+2\sigma & \dots & 0 & 0 \\ \dots & \dots & \dots & \dots & \dots & \dots \\ -\sigma & 0 & 0 & \dots & -\sigma & 1+2\sigma \end{bmatrix} \quad (1)$$

for some $\sigma \geq 0$. The resulting Laplacian smoothing stochastic gradient descent (LS-SGD) requires negligible extra computational cost and generalizes better than the standard SGD. When the Hessian has a poor condition number, gradient descent performs poorly. In this case, the derivative increases rapidly in one direction, while increasing slowly in others. Gradient smoothing can avoid jitter along steep directions and help make progress in shallow directions. Our proposed approach is linked to an unusual HJ-PDE whose solution convexifies the original loss function while retaining its flat (and global) minima, and we essentially work on this surrogate function with a much better landscape.

This paper is structured in the following way: in section 2, we build the connection between minimizing a nonconvex function and solving a class of HJ-PDEs. In section 3, we present the efficient flat minima searching algorithm which we call Laplacian smoothing gradient descent (LS-GD), and discuss its convergence. In section 4, we validate the efficiency of the new algorithm by performing various machine learning tasks, ranging from softmax regression to convolutional neural nets (CNNs) to generative adversarial nets (GANs), to deep reinforcement learning (DRL). The summary and future work are given in section 5. The technical proofs are provided in the appendix.

2 Flat Minima and Hamilton-Jacobi PDEs

Machine learning problems are generally formulated as finding the optimal parameters \mathbf{w} of a parametric function $\mathbf{y} = f(\mathbf{x}, \mathbf{w})$, such that for a given input \mathbf{x} , the output \mathbf{y} is as accurate as possible. The optimal parameters \mathbf{w} can be obtained by minimizing an empirical risk function, $\mathcal{L}(X, Y, \mathbf{w}) \doteq \mathcal{L}(\mathbf{w})$, given the training data $\{X, Y\}$.

We consider the problem of finding a global or at least flat minima of $\mathcal{L}(\mathbf{w})$. To this end, we introduce the following unusual HJ-PDE with $\mathcal{L}(\mathbf{w})$ as initial condition

$$\begin{cases} u_t + \frac{1}{2} \langle \nabla_{\mathbf{w}} u, A_\sigma^{-1} \nabla_{\mathbf{w}} u \rangle = 0, & (\mathbf{w}, t) \in \Omega \times [0, \infty) \\ u(\mathbf{w}, 0) = \mathcal{L}(\mathbf{w}), & \mathbf{w} \in \Omega \end{cases} \quad (2)$$

where A is given in (1). Ω is the domain, and $\sigma > 0$ is a parameter. By the Hopf-Lax formula [9], the unique viscosity solution to the above problem can be represented by

$$u(\mathbf{w}, t) = \inf_{\mathbf{v}} \left\{ \mathcal{L}(\mathbf{v}) + \frac{1}{2t} \langle \mathbf{v} - \mathbf{w}, A_\sigma(\mathbf{v} - \mathbf{w}) \rangle \right\}.$$

This viscosity solution $u_t(\mathbf{w}) := u(\mathbf{w}, t)$ convexifies $\mathcal{L}(\mathbf{w})$ by bringing down the local maxima while retaining the wide minima. An illustration of this convexification procedure is shown in Fig. 1. If we perform the smoothing GD with proper step size on the convexified function $u_t(\mathbf{w})$, it is easier to reach the global or at least a flat minima of the original nonconvex function $\mathcal{L}(\mathbf{w})$.

Proposition 1. *Suppose $\mathcal{L}(\mathbf{w})$ is convex, the Laplacian smoothing GD on $u_t(\mathbf{w})$*

$$\mathbf{w}^{k+1} = \mathbf{w}^k - t A_\sigma^{-1} \nabla u_t(\mathbf{w}^k)$$

is equivalent to the smoothing implicit gradient descent on $\mathcal{L}(\mathbf{w})$

$$\mathbf{w}^{k+1} = \mathbf{w}^k - t A_\sigma^{-1} \nabla \mathcal{L}(\mathbf{w}^{k+1}).$$

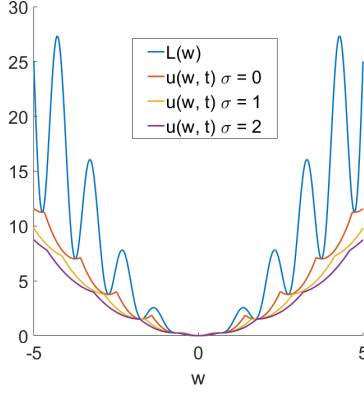


Figure 1: Convexification of $\mathcal{L}(\mathbf{w}) = \|\mathbf{w}\|^2(1 + 0.5 \sin(2\pi\|\mathbf{w}\|))$ by Laplacian smoothing (viscosity solutions of HJ-PDE Eq.(2)). The plot shows the cross section of a 5-D problem with $t = 0.1$ and different σ values.

3 Algorithm and Analysis

Laplacian smoothing implicit gradient descent requires inner iterations as used in [7], which is computationally expensive. We propose to relax the implicit scheme into the following explicit scheme

$$\mathbf{w}^{k+1} = \mathbf{w}^k - \gamma_k A_\sigma^{-1} \nabla \mathcal{L}(\mathbf{w}^k) \doteq \mathbf{w}^k - \gamma_k \nabla^\sigma \mathcal{L}(\mathbf{w}^k).$$

Intuitively, compared to the standard GD, this scheme smooths the gradient on-the-fly by an elliptic smoothing operator. In the discrete case, ∇^σ with periodic boundary condition is simply the inverse of the tri-diagonal matrix defined in (1).

The inverse of this tri-diagonal matrix can be found with linear time complexity by using the Thomas algorithm together with the Sherman–Morrison formula. Here instead we adopt an efficient fast Fourier transform (FFT) implementation that is available in both PyTorch [25] and TensorFlow [1]. Given a vector \mathbf{a} , a smoothed vector \mathbf{b} can be obtained by solving $A_\sigma^{-1} \mathbf{a} = \mathbf{b}$. This is equivalent to $\mathbf{a} = \mathbf{b} - \sigma \mathbf{v} * \mathbf{b}$, where $\mathbf{v} = (-2, 1, 0, \dots, 0, 1)$ and $*$ is the convolutional operator. Hence, we have

$$\mathbf{b} = \text{ifft} \left(\frac{\text{fft}(\mathbf{a})}{1 - \sigma \cdot \text{fft}(\mathbf{v})} \right),$$

where fft and ifft are the FFT and inverse FFT operations, respectively. Therefore, the smoothed gradient can be obtained in quasilinear time. This additional time complexity is almost the same as performing a one step update on the weights vector \mathbf{w} . For many machine learning models, we may need to concatenate the parameters into a vector. This reshape might lead to some ambiguity, nevertheless, based on our tests, both row and column majored reshaping work for LS-GD algorithm. Moreover, in deep learning cases, the weights in different layers might have different physical meanings. We then perform layer-wise gradient smoothing, instead.

3.1 Circumvent Sharp Minima

To explicitly show that the LS-GD helps to bypass sharp minima and reach flat minima, we consider the following function, in which we ‘drill’ narrow holes on a smooth convex function,

$$f(x, y, z) = -4e^{-((x-\pi)^2 + (y-\pi)^2 + (z-\pi)^2)} - 4 \sum_i \cos(x) \cos(y) e^{-\beta((x-r \sin(\frac{i}{2})) - \pi)^2 + (y-r \cos(\frac{i}{2}) - \pi)^2)} \quad (3)$$

where the summation is taken over the index set $\{i \in \mathbb{N} | 0 \leq i < 4\pi\}$, r and β are the parameters that determine the location and narrowness of the local minima and are set to 1 and $\frac{1}{\sqrt{500}}$, respectively. We do GD with regular and Laplacian smoothed gradient starting from a random point in the neighborhoods of the narrow minima, i.e., $x_0 \in \{\bigcup_i U_\delta(r \sin(\frac{i}{2}) + \pi, r \cos(\frac{i}{2}) + \pi) | 0 \leq i < 4\pi, i \in \mathbb{N}\}$, where $U_\delta(P)$ is a neighborhood of the point P with radius δ . Our experiments (Fig. 2) show that, if $\delta \leq 0.2$, GD with the raw gradient will converge to narrow local minima, while the convergence to wider global minima is obtained by using the smoothed surrogate.

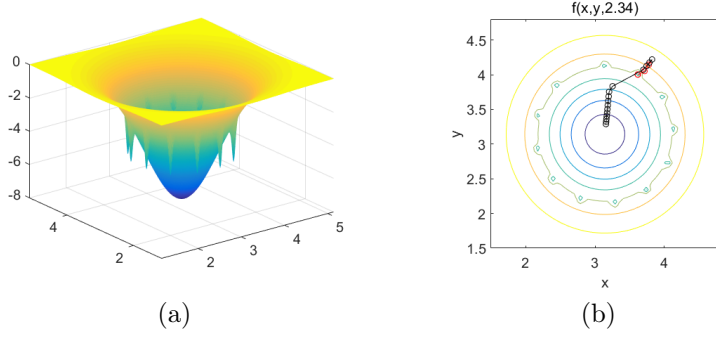


Figure 2: Demo of gradient descent with raw and Laplacian smoothed gradients. Panel (a) depicts a slice of the function, $z = 2.34$, given by Eq.(3); panel (b) shows the paths by using two different gradients, where red and black dots are the sampled points on the paths with raw and smoothed gradients, respectively. The learning rate in the gradient descent is set to be 0.02 and the smoothing parameter $\sigma = 1.0$.

3.2 Analysis of LS-GD

It is easy to see that the Laplacian smoothing has the following two properties:

Proposition 2 (The Min-Max Principle). *For any vector $\mathbf{g} \in \mathbb{R}^n$, we have $\min_i (A_\sigma^{-1} \mathbf{g})_i \geq \min_i \mathbf{g}_i$ and $\max_i (A_\sigma^{-1} \mathbf{g})_i \leq \max_i \mathbf{g}_i$, where \mathbf{g}_i is the i th component of the vector \mathbf{g} . In particular, we have $\min_i (\nabla^\sigma \mathcal{L}(\mathbf{w}))_i \geq \min_i (\nabla \mathcal{L}(\mathbf{w}))_i$ and $\max_i (\nabla^\sigma \mathcal{L}(\mathbf{w}))_i \leq \max_i (\nabla \mathcal{L}(\mathbf{w}))_i$.*

Proposition 3 (Conversation Law). *The operator A_σ^{-1} preserves the sum of components for all $\sigma > 0$. For any $\mathbf{g} \in \mathbb{R}^n$, we have $\sum_i (A_\sigma^{-1} \mathbf{g})_i = \sum_i \mathbf{g}_i$. In particular,*

$$\sum_i (\nabla^\sigma \mathcal{L}(\mathbf{w}))_i = \sum_i (\nabla \mathcal{L}(\mathbf{w}))_i.$$

The above results imply that the operator A_σ^{-1} indeed smooths the gradient with smaller (in magnitude) extreme components. Next, we analyze the convergence for a class of algorithms including the LS-GD algorithm.

Proposition 4. *Suppose $\nabla \mathcal{L}(\mathbf{w})$ is L -Lipschitz continuous. Let $\{\mathbf{w}^k\}$ be generated by LS-GD, and let $\lambda_{\min}, \lambda_{\max} > 0$ be the smallest and largest eigenvalues of A_σ^{-1} , respectively. Suppose $\underline{\gamma} \leq \gamma_k \leq \bar{\gamma} < \frac{2\lambda_{\min}}{\lambda_{\max}^2 L}$ for some $\underline{\gamma}, \bar{\gamma} > 0$. Then we have*

$$\lim_{k \rightarrow \infty} \|\nabla \mathcal{L}(\mathbf{w}^k)\| = 0.$$

It is not hard to see that similar convergence result holds for the stochastic case, under extra assumptions on the sampled gradient.

4 Numerical Results

4.1 Softmax Regression

We consider the MNIST hand written digits [18] recognition by using the softmax regression as classifier. The models are trained by running 100 epochs of SGD and LS-SGD respectively on the 60000 training instances with batch size 100 and learning rate 0.05. Results shown in Fig. 3 and Table 1 show that compared to SGD, LS-SGD dramatically reduces the variance and meanwhile improves the accuracy of generalization. It is seen that SGD might train the model that has generalization accuracy less than 90% while LS-SGD with $\sigma = 0.8$ gives the generalization accuracy always above 91.5% over 100 independent trials.

4.2 LeNet for MNIST Recognition

We consider LeNet [19] for MNIST classification. Our network architecture is as follows

$$\text{LeNet} : \text{input}_{28 \times 28} \rightarrow \text{conv}_{20,5,2} \rightarrow \text{conv}_{50,5,2} \rightarrow \text{fc}_{512} \rightarrow \text{softmax}.$$

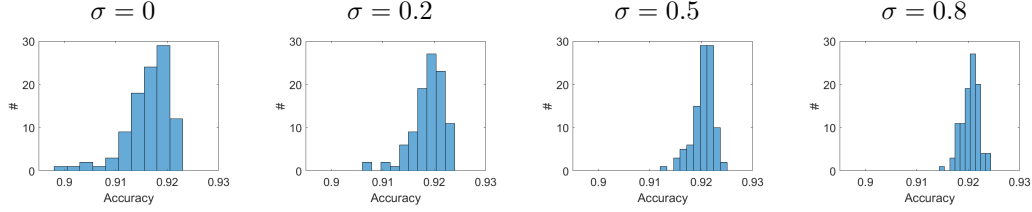


Figure 3: The histogram of generalization accuracies of the softmax regression model trained with LS-SGD over 100 independent experiments by using different σ . Note, $\sigma = 0$ represents SGD.

Table 1: Accuracies of the softmax regression model trained with LS-SGD. Statistics over 100 independent experiments for each σ . Note, $\sigma = 0$ represents SGD.

σ	Min	Max	Average	Variance	σ	Min	Max	Average	Variance
0.0	0.8987	0.9226	0.9163	1.8107e-5					
0.1	0.9064	0.9243	0.9180	1.0991e-5	0.6	0.9167	0.9250	0.9207	3.1738e-6
0.2	0.9065	0.9239	0.9189	1.0572e-5	0.7	0.9152	0.9243	0.9206	3.3016e-6
0.3	0.9082	0.9244	0.9197	8.1568e-6	0.8	0.9153	0.9244	0.9205	2.7335e-6
0.4	0.9098	0.9253	0.9197	7.4750e-6	0.9	0.9165	0.9241	0.9204	2.7965e-6
0.5	0.9120	0.9241	0.9204	4.2096e-6	1.0	0.9135	0.9244	0.9203	3.8587e-6

The notation $\text{conv}_{c,k,m}$ denotes a 2D convolutional layer with c output channels, each of which is the sum of a channel-wise convolution operation on the input using a learnable kernel of size $k \times k$, it further adds ReLU nonlinearity and max pooling with stride size m . fc_{512} is an affine transformation that transforms the input to a vector of dimension 512. Finally, the tensors are activated by a softmax function. The MNIST data is first passed to the layer $\text{input}_{28 \times 28}$, and further processed by this hierarchical structure. We compare the performances of SGD and LS-SGD.

We first consider LS-SGD with different σ and without any extra thrust, e.g., momentum. We train the model by running 100 epochs LS-SGD with learning rate 0.05 and batch size 100. Fig. 4 plots the distribution of the generalization accuracy over 100 independent experiments. Compared to SGD ($\sigma = 0.0$), with $\sigma = 1.0$, the generalization accuracy of LS-SGD peaked at a better place. Furthermore, the best generalization accuracy increases from 0.9911 to 0.9917. We list the detailed results in Table 2.

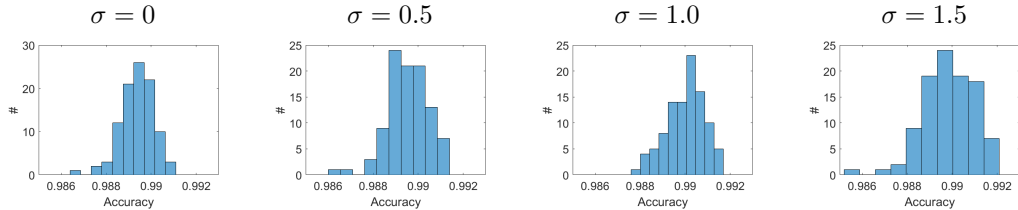


Figure 4: The histogram of generalization accuracies of the LeNet on MNIST trained with LS-SGD over 100 independent experiments by using different σ . Neither momentum, nor weight decay, nor any other techniques is used to improve the generalization. Note, $\sigma = 0$ represents SGD.

Table 2: Accuracies of the LeNet trained with LS-SGD. Statistics over 100 independent experiments for each σ . Note, $\sigma = 0$ recovers SGD.

σ	Min	Max	Average	Variance	σ	Min	Max	Average	Variance
0.0	0.9864	0.9911	0.9894	6.3563e-7	1.0	0.9876	0.9917	0.9900	5.2606e-7
0.5	0.9895	0.9914	0.9895	8.1497e-7	1.5	0.9865	0.9921	0.9898	1.2920e-6

Many simple yet elegant optimization techniques are introduced to SGD to improve both training and generalization of the DNNs, including Nesterov momentum [28], weight decay [17], etc. We further compare the performance of LS-SGD when these techniques are applied. We run 100 epochs of both SGD and LS-SGD with initial learning rate 0.01 and divide by 5 after 50 epochs, and use a weight decay of 0.0001 and momentum of 0.9. The batch size remains at 100. In LS-SGD, we set $\sigma = 1.0$. Figure. 5 plots the accuracy distributions over 100 experiments with SGD and LS-SGD. It is seen that the advantage of LS-SGD is preserved. Moreover, in a few cases, the model trained by SGD has generalization accuracy less than 0.991 while this never happens if LS-SGD is applied. We believe this might be related to the fact that LS-SGD successfully bypasses sharp minima which generalizes less accurately. And LS-SGD has chances to converge to a minima with better generalization.

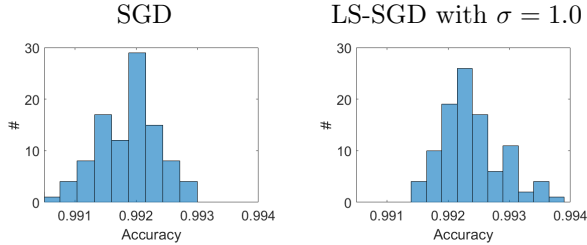


Figure 5: The histogram of generalization accuracies of the LeNet on MNIST trained with LS-SGD over 100 independent experiments by using different σ . Nesterov momentum and weight decay are used to boost the performance.

4.3 ResNet for Cifar10 Classification

The skip connections in ResNet smooths the landscape of the loss function of the classical CNN [13, 20]. This means that ResNet has fewer sharp minima. On Cifar10 [16], we compare the performance of LS-SGD and SGD on ResNet with the pre-activated ResNet56 as an illustration. We take the same training strategy as that used in [13], except that we run 200 epochs with the learning rate decaying by a factor of 5 after every 40 epochs. For ResNet, instead of applying LS-SGD for all epochs, we only use LS-SGD in the first 40 epochs, and the remaining training is carried out by SGD. The parameter σ is set to 1.0. Figure 6 depicts one path of the training and generalization accuracies of the neural nets trained by SGD and LS-SGD, respectively. It is seen that, even though the training accuracy by SGD is higher than that by LS-SGD, the generalization is however inferior to that of LS-SGD. We conjecture that, this is due to the fact that SGD gets trapped into some sharp but deeper minimum, which fits better than a flat minimum but generalizes worse. We carry out 25 replicas of this experiments, the histograms of the corresponding accuracies are shown in Fig. 7.

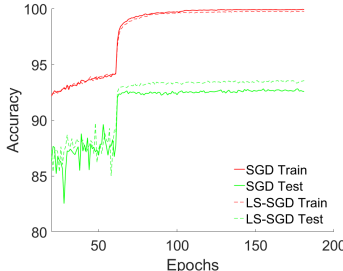


Figure 6: The evolution of the pre-activated ResNet56’s training and generalization accuracies by SGD and LS-SGD. (Start from the 20-th epoch.)

4.4 Wasserstein GAN Optimization

Generative Adversarial Networks (GANs) [11] are notoriously delicate and unstable to train [2]. In [21], Wasserstein-GANs (WGANs) are introduced to combat the instability in the training

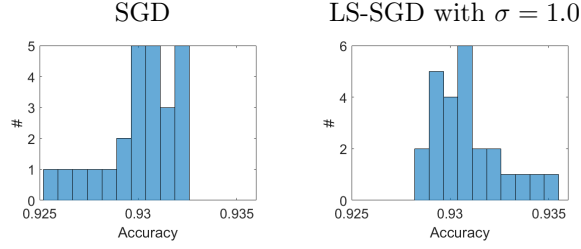


Figure 7: The histogram of the generalization accuracies of the pre-activated ResNet56 on Cifar10 trained with LS-SGD over 25 independent experiments.

of GANs. In addition to being more robust in training parameters and network architecture, WGANs provide a reliable estimate of the Earth Mover (EM) metric which correlates well with the quality of the generated samples. Nonetheless, WGAN training becomes unstable with a large learning rate or when used with a momentum based optimizer [21]. In this section, we demonstrate that the gradient smoothing technique in this paper alleviates the instability in the training, and improves the quality of generated samples. Since WGANs with weight clipping are typically trained with RMSProp [29], we propose replacing the gradient g by a smoothed version $g_\sigma = (I - \sigma\Delta)^{-1}g$, and also update the running averages using g_σ instead of g . We name this algorithm LS-RMSProp.

To accentuate the instability in training and demonstrate the effects of gradient smoothing, we deliberately use a large learning rate for training the generator. We compare the regular RMSProp with the proposed LS-RMSProp. The learning rate for the critic is kept small and trained approximately to convergence so that the critic loss is still an effective approximation to the Wasserstein distance. To control the number of unknowns in the experiment and make a meaningful comparison using the critic loss, we use the classical RMSProp for the critic, and only apply LS-RMSProp to the generator.

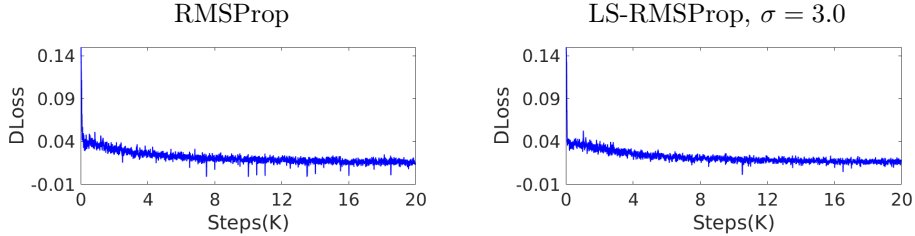


Figure 8: Critic Loss with learning rate $lr_D = 0.0001$, $lr_G = 0.005$ for RMSProp (Left) and LS-RMSProp (Right), trained for 20K iterations. We apply a mean filter of window size 13 for better visualization. The loss from LS-RMSProp is visibly less noisy.

We train the WGAN on the MNIST dataset using the DCGAN architecture [26] for both the critic and generator. In Figure 8 (left), we observe the loss for RMSProp trained with a large learning rate has multiple sharp spikes, indicating instability in the training process. The samples generated are also lower in quality, containing noisy spots as shown in Figure 9 (left). In contrast, the curve of training loss for LS-RMSProp is smoother and exhibits fewer spikes. The generated samples as shown in Figure 9 (right) are also of better quality and visibly less noisy. A reasonable conjecture for this improved stability is that the spikes which appear in training for RMSProp correspond to sharp extrema in the approximate EM metric, and this is circumvented by smoothing the gradient. The effects are less pronounced with a small learning rate, but still result in a modest improvement in sample quality as shown in Figure 10. We also apply LS-RMSProp for training the critic, but do not see a clear improvement in the quality. This may be because the critic is already trained near optimality during each iteration, and does not benefit much from gradient smoothing.

4.5 Deep Reinforcement Learning

Recently, DRL has been successfully applied to playing games including Cartpole [5], Atari [23], Go [27, 22]. DNNs play a vital role in approximating the Q-function or policy function in DRL.

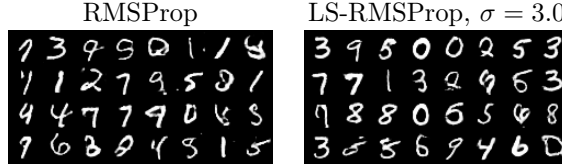


Figure 9: Samples from WGAN trained with RMSProp (left) and LS-RMSProp (right). The learning rate is set to $lr_D = 0.0001$, $lr_G = 0.005$ for both RMSProp and LS-RMSProp. The critic is trained for 5 iterations per every step of the generator, and 200 iterations per every 500 steps of the generator.

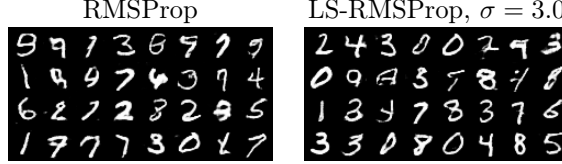


Figure 10: Samples from WGAN trained with RMSProp (left) and LS-RMSProp (right). The learning rate is set to $lr_D = 0.0001$, $lr_G = 0.0001$ for both RMSProp and LS-RMSProp. The critic is trained for 5 iterations per every step of the generator, and 200 iterations per every 500 steps of the generator.

We apply the Laplacian smoothed gradient to train the policy function to play Cartpole game. We follow the standard procedure to train the policy function by using the policy gradient [5]. We use the following very simple network to approximate the policy function:

$$\text{input}_4 \rightarrow \text{fc}_{20} \rightarrow \text{relu} \rightarrow \text{fc}_2 \rightarrow \text{softmax}.$$

The network is trained by RMSProp and LS-RMSProp with $\sigma = 1.0$, respectively. The learning rate and other related parameters are set to be the default ones in PyTorch. The training is stopped once the average duration of 5 consecutive episodes is more than 490. In each training episode, we set the maximal steps to be 500. Left and right panels of Fig. 11 depict a training procedure by using RMSProp and LS-RMSProp, respectively. We see that Laplacian smoothed gradient takes fewer episodes to reach the stopping criterion. Moreover, we ran the above experiments 5 times independently, and applied the trained model to play Cartpole. The game lasted more than 1000 steps for all the 5 models trained by LS-RMSProp, while only 3 of them lasted more than 1000 steps when the model is trained by vanilla RMSProp.

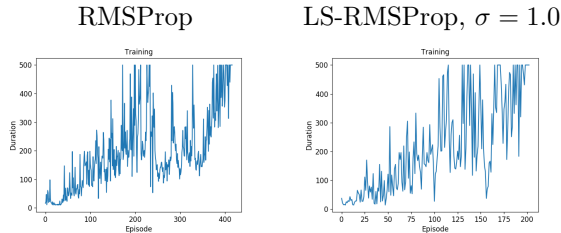


Figure 11: Durations of the cartpole game in the training procedure. Left and right are training procedure by RMSProp and LS-RMSProp with $\sigma = 1.0$, respectively.

5 Concluding Remarks

In order to find the global or flat minima on the complex nonconvex landscape, we take the idea from Hamilton-Jacobi partial differential equation and proposed the Laplacian smoothing gradient descent algorithm. In contrast to the previous algorithms which mainly consider the local geometry around the sharp minima, we took advantage of information revealed from the gradient. Therefore our algorithm is essentially of the same complexity as gradient descent. Extensive numerical examples ranging from toy cases to shallow and deep neural nets to generative

adversarial networks and to deep reinforcement learning, all demonstrate the advantage of the proposed smoothed gradient. The convergence of the smooth gradient descent was proved. Several issues remain including gradient smoothing by solving the tri-diagonal matrix instead of using fast Fourier transform; and on-the-fly adaptive method for choosing smoothing parameters σ instead of using a fixed value.

Acknowledgments

This material is based on research sponsored by the Air Force Research Laboratory and DARPA under agreement number FA8750-18-2-0066. And by the U.S. Department of Energy, Office of Science and by National Science Foundation, under Grant Numbers DOE-SC0013838 and DMS-1554564, (STROBE). And by the NSF DMS-1737770 and the Simons foundation. The U.S. Government is authorized to reproduce and distribute reprints for Governmental purposes notwithstanding any copyright notation thereon.

References

- [1] M. Abadi, A. Agarwal, and et al. Tensorflow: Large-scale machine learning on heterogeneous distributed systems. [arXiv:1603.04467](#), 2016.
- [2] M. Arjovsky and L. Bottou. Towards principled methods for training generative adversarial networks. [arXiv preprint arXiv:1701.04862](#), 2017.
- [3] L. Bottou, E. Frank, and J. Nocedal. Optimization methods for large-scale machine learning. [arXiv preprint arXiv:1606.04838](#), 2016.
- [4] O. Bousquet and A. Elisseeff. Stability and generalization. [Journal of Machine Learning Research](#), 2:499–526, 2002.
- [5] G. Brockman, V. Cheung, L. Pettersson, J. Schneider, J. Schulman, J. Tang, and W. Zaremba. Openai gym. [arXiv:1606.01540](#), 2016.
- [6] P. Chaudhari, A. Choromanska, S. Soatto, Y. LeCun, C. Baldassi Carlo, C. Borgs, J. Chayes, L. Sagun, and R. Zecchina. Entropy-sgd: Biasing gradient descent into wide valleys. [arXiv preprint arXiv:1611.01838](#), 2016.
- [7] P. Chaudhari, A. Oberman, S. Osher, S. Soatto, and C. Guillame. Deep relaxation: partial differential equations for optimizing deep neural networks. [arXiv preprint arXiv:1704.04932](#), 2017.
- [8] J. Duchi, E. Hazan, and Y. Singer. Adaptive subgradient methods for online learning and stochastic optimization. [Journal of Machine Learning Research](#), 12:2121–2159, 2011.
- [9] L.C. Evans. Partial differential equations. [American Mathematical Soc](#), 2010.
- [10] A. Gonen and S. Shalev-Shwartz. Fast rates for empirical risk minimization of strict saddle problems. [arXiv preprint arXiv:1701.04271](#), 2017.
- [11] I. J. Goodfellow, J. Pouget-Abadie, M. Mirza, B. Xu, D. Warde-Farley, S. Ozair, A. C. Courville, and Y. Bengio. Generative adversarial nets. [Advances in Neural Information Processing Systems](#), pages 2672–2680, 2014.
- [12] M. Hardt, B. Recht, and Y. Singer. Train faster, generalize better: Stability of stochastic gradient descent. In [International Conference on Learning Representations](#), 2016.
- [13] K. He, X. Zhang, S. Ren, and J. Sun. Deep residual learning for image recognition. [CVPR](#), pages 770–778, 2016.
- [14] S. Jastrzebski, Z. Kenton, N. Ballas, A. Fischer, Y. Bengio, and A. Storkey. Sgd smooths the sharpest directions. In [International Conference on Learning Representations](#), 2018.
- [15] N. Keskar, M. Shirish, N. Dheevatsa, S. Jorge, Mikhail, P. Tang, and P. Tak. On large-batch training for deep learning: Generalization gap and sharp minima. [arXiv preprint arXiv:1609.04836](#), 2017.
- [16] A. Krizhevsky. Learning multiple layers of features from tiny images. 2009.
- [17] A. Krogh and J. A. Hertz. A simple weight decay can improve generalization. [Advances in Neural Information Processing Systems](#), pages 950–957, 1992.
- [18] Y. LeCun. The mnist database of handwritten digits. 1998.

- [19] Y. LeCun, L. Bottou, Y. Bengio, and P. Haffner. Gradient-based learning applied to document recognition. Proceedings of the IEEE, 81:2278–2324, 1998.
- [20] H. Li, Z. Xu, G. Taylor, and T. Goldstein. Visualizing the loss landscape of neural nets. In Deep Learning: Bridging Theory and Practice, NIPS Workshop, 2017.
- [21] S. Chintala M. Arjovsky and L. Bottou. Wasserstein gan. arXiv preprint arXiv:1701.07875, 2017.
- [22] Mnih and et al. Human-level control through deep reinforcement learning. Nature, 518:529–533, 2015.
- [23] V. Mnih, K. Kavukcuoglu, D. Silver, A. Graves, I. Antonoglou, D. Wierstra, and M. Riedmiller. Playing Atari with deep reinforcement learning. arXiv:1312.5602, 2013.
- [24] J.-J. Moreau. Proximité et dualité dans un espace hilbertien. Bulletin de la Société Mathématique de France, 93:273–299, 1965.
- [25] A. Paszke, S. Gross, S. Chintala, G. Chanan, E. Yang, Z. DeVito, Z. Lin, A. Desmaison, L. Antiga, and A. Lerer. Automatic differentiation in pytorch. 2017.
- [26] A. Radford, L. Metz, and S. Chintala. Unsupervised representation learning with deep convolutional generative adversarial networks. arXiv preprint arXiv:1511.06434, 2015.
- [27] D. Silver and et al. Mastering the game of go with deep neural networks and tree search. Nature, 529:484–489, 2016.
- [28] I. Sutskever, J. Martens, G. Dahl, and G. Hinton. On the importance of initialization and momentum in deep learning. In International Conference on Machine Learning, 2013.
- [29] T. Tieleman and G. Hinton. Lecture 6.5-rmsprop: Divide the gradient by a running average of its recent magnitude. COURSERA: Neural networks for machine learning, 4(2):26–31, 2012.
- [30] P. Yin, M. Pham, A. Oberman, and S. Osher. Stochastic backward euler: An implicit gradient descent algorithm for k-means clustering. UCLA CAM Report 17-57, 2017.

Appendix

Proof of Proposition 1. We denote $A := \mathcal{I} - \sigma\Delta$ and $\|\cdot\|_A := \langle \cdot, A\cdot \rangle$.

$$u_t(\mathbf{w}) = \inf_{\mathbf{v}} \left\{ \mathcal{L}(\mathbf{v}) + \frac{1}{2t} \|\mathbf{v} - \mathbf{w}\|_A^2 \right\}. \quad (4)$$

Since the biconjugate of $u_t(\mathbf{w})$ is itself, we have

$$u_t(\mathbf{w}) = u_t^{**}(\mathbf{w}) = (u_t^*(\mathbf{v}))^* = \sup_{\mathbf{v}} \left\{ \mathbf{w}^\top \mathbf{v} - u_t^*(\mathbf{v}) \right\} = \sup_{\mathbf{v}} \left\{ \mathbf{w}^\top \mathbf{v} - \mathcal{L}^*(\mathbf{v}) - \frac{t}{2} \|\mathbf{v}\|_{A^{-1}}^2 \right\}.$$

In the last equality above, we used the infimal convolution:

$$u_t^*(\mathbf{v}) = \mathcal{L}^*(\mathbf{v}) + \left(\frac{1}{2t} \|\cdot\|_A^2 \right)^*(\mathbf{v}) = \mathcal{L}^*(\mathbf{v}) + \frac{t}{2} \|\mathbf{v}\|_{A^{-1}}^2.$$

Then $\nabla u_t(\mathbf{w}) = \arg \max_{\mathbf{v}} \left\{ \mathbf{w}^\top \mathbf{v} - \mathcal{L}^*(\mathbf{v}) - \frac{t}{2} \|\mathbf{v}\|_{A^{-1}}^2 \right\}$. Therefore, by the optimality condition,

$$\mathbf{w} - tA^{-1}\nabla u_t(\mathbf{w}) \in \partial \mathcal{L}^*(\nabla u_t(\mathbf{w})),$$

which is equivalent to

$$\nabla u_t(\mathbf{w}) \in \partial \mathcal{L}(\mathbf{w} - tA^{-1}\nabla u_t(\mathbf{w})). \quad (5)$$

Let $\mathbf{z} = \mathbf{w} - tA^{-1}\nabla u_t(\mathbf{w})$. Then (5) reduces to

$$\frac{1}{t}A(\mathbf{w} - \mathbf{z}) \in \partial \mathcal{L}(\mathbf{z})$$

and thus $\mathbf{z} = \mathbf{w} - tA^{-1}\nabla \mathcal{L}(\mathbf{z})$. \square

Proof of Proposition 2. Let $\mathbf{h} = (\mathcal{I} - \sigma\Delta)^{-1}\mathbf{g}$, then $\mathbf{g} = (\mathcal{I} - \sigma\Delta)\mathbf{h}$. Suppose $p = \arg \min_i \mathbf{h}_i$, it holds that

$$\mathbf{g}_p = \mathbf{h}_p + \sigma(2\mathbf{h}_p - \mathbf{h}_{p-1} - \mathbf{h}_{p+1}),$$

where periodicity of subindex are used if necessary. Since $2\mathbf{h}_p - \mathbf{h}_{p-1} - \mathbf{h}_{p+1} \leq 0$, we have $\min_i \mathbf{g}_i \leq \mathbf{g}_p \leq \mathbf{h}_p = \min_i \mathbf{h}_i$. Similar arguments can show that $\max_i \mathbf{g}_i \geq \max_i \mathbf{h}_i$. \square

Proof of Proposition 3. Let $\mathbf{h} = (\mathcal{I} - \sigma\Delta)^{-1}\mathbf{g}$, then $\mathbf{g} = (\mathcal{I} - \sigma\Delta)\mathbf{h} = \mathbf{h} - \sigma\Delta\mathbf{h}$. Then

$$\sum_i \mathbf{g}_i = \mathbf{1}^\top \mathbf{g}_i = \mathbf{1}^\top (\mathbf{h} - \sigma\Delta\mathbf{h}) = \mathbf{1}^\top \mathbf{h} = \sum_i \mathbf{h}_i,$$

where we used $\mathbf{1}^\top \Delta = \mathbf{0}^\top$. \square

Proof of Proposition 4. For notational convenience, let us define $H := (\mathcal{I} - \sigma\Delta)^{-1}$. Since \mathcal{L} is L -Lipschitz differentiable, we have

$$\begin{aligned} \mathcal{L}(\mathbf{w}^{k+1}) &= \mathcal{L}(\mathbf{w}^k - \gamma_k H \nabla \mathcal{L}(\mathbf{w}^k)) \leq \mathcal{L}(\mathbf{w}^k) - \gamma_k \langle \nabla \mathcal{L}(\mathbf{w}^k), H \nabla \mathcal{L}(\mathbf{w}^k) \rangle + \frac{L\gamma_k^2}{2} \|H \nabla \mathcal{L}(\mathbf{w}^k)\|^2 \\ &\leq \mathcal{L}(\mathbf{w}^k) - \gamma_k \lambda_{\min} \|\nabla \mathcal{L}(\mathbf{w}^k)\|^2 + \frac{\lambda_{\max}^2 L \gamma_k^2}{2} \|\nabla \mathcal{L}(\mathbf{w}^k)\|^2. \end{aligned}$$

Summing up the above inequalities and re-arranging the terms, we have

$$\sum_{k=0}^{N-1} \left(\lambda_{\min} \gamma_k - \frac{\lambda_{\max}^2 L \gamma_k^2}{2} \right) \|\nabla \mathcal{L}(\mathbf{w}^k)\|^2 \leq \mathcal{L}(\mathbf{w}^0) - \mathcal{L}(\mathbf{w}^N).$$

Letting $N \rightarrow \infty$, we have

$$\gamma \left(\lambda_{\min} - \frac{\lambda_{\max}^2 L \bar{\gamma}}{2} \right) \sum_{k=0}^{\infty} \|\nabla \mathcal{L}(\mathbf{w}^k)\|^2 \leq \sum_{k=0}^{\infty} \left(\lambda_{\min} \gamma_k - \frac{\lambda_{\max}^2 L \gamma_k^2}{2} \right) \|\nabla \mathcal{L}(\mathbf{w}^k)\|^2 < \infty.$$

Using $\lambda_{\min} - \frac{\lambda_{\max}^2 L \bar{\gamma}}{2} > 0$, we have

$$\sum_{k=0}^{\infty} \|\nabla \mathcal{L}(\mathbf{w}^k)\|^2 < \infty.$$

We must have $\lim_{k \rightarrow \infty} \|\nabla \mathcal{L}(\mathbf{w}^k)\|^2 = 0$. \square